Available online at www.sciencedirect.com
SCIENCE DIRECT®
Chemical Physics Letters 366 (2002) 642–649
CHEMICAL PHYSICS LETTERS
www.elsevier.com/locate/cplett

Dissociation dynamics and stability of cyclopentoxy and cyclopentoxide

Leah S. Alconcel, Robert E. Continetti *

Department of Chemistry and Biochemistry, 0340 University of California, San Diego, 9500 Gilman Drive, La Jolla, CA 92093-0340, USA

Received 25 July 2002; in final form 4 October 2002

Abstract

Cyclopentoxide c-$C_5H_9O^-$ undergoes photodetachment to stable cyclopentoxy or the ring-opened 5-oxo-pentan-1-yl radical and dissociative photodetachment, yielding C_3H_5O and C_2H_4 photofragments, at both 532 and 355 nm. The adiabatic electron affinity of c-$C_5H_9O^-$ is estimated from the experimental results and ab intio calculations to be 1.5 ± 0.1 eV. The results show that c-$C_5H_9O^-$ is stable relative to dissociation into $C_3H_5O^-$ and C_2H_4 by 1.23 ± 0.07 eV, whereas c-C_5H_9O is unstable relative to C_3H_5O and C_2H_4 by -0.12 ± 0.12 eV. These results are discussed in terms of the factors affecting the stability of cyclic alkoxides and the corresponding alkoxy radicals.

1. Introduction

The importance of alkoxy radicals in atmospheric chemistry is well established. These species participate as intermediates in the formation of tropospheric ozone and it is known that they may undergo unimolecular dissociation to produce other reactive species [1]. Identifying trends in the dependence of the energetics and dynamics of alkoxy species on the type and size of the alkyl moiety assists in understanding their reactivity.

Many theoretical and experimental studies have been devoted to the electronic structures of small cycloalkane species, since the bond angles, bond lengths and torsional angles in these molecules deviate from the optimal values [2–13]. Parsing the competing forces in strained molecules is a complex problem. The high angle strain (60° bond angles) in cyclopropane is mitigated by the configuration of the bonding orbitals, which are hybridized like the bonds in unsaturated hydrocarbons (sp^2) and do not lie along the bond angles [2,3,5,7–11]. Although the angle strain in nonplanar cyclobutane is reduced, the torsional strain is higher and the ring bonding orbitals do not overlap as well as in cyclopropane [4,6,9,10,14]. Due to these and other contributing factors, the overall ring strain energies of the two smallest cycloalkanes are similar [4,12,14]. In contrast, the ring strain in cyclopentane is drastically reduced [4,12,14]. The bond angles are nearly tetrahedral, obviating the need for the unusual bonding

* Corresponding author. Fax: +1-858-534-7244.
E-mail address: rcontinetti@ucsd.edu (R.E. Continetti).

0009-2614/02/$ - see front matter
PII: S0009-2614(02)01633-0

configuration observed in cyclopropane [15]. Despite ring puckering [15,16], torsional strain remains since the CH bonds are not totally eclipsed [4,14]. Substituting an oxygen atom for one of the hydrogens in a cycloalkane ring puts the oxygen lone pairs in close proximity to the ring orbitals. Photodetachment studies of cyclic alkoxides provide a way to probe the interaction between the oxygen and the cycloalkyl moiety.

The strain in small cycloalkyl moieties strongly affects the photodetachment processes of the cyclic alkoxy species studied previously in this laboratory [17]. In these studies, cyclopropoxide and cyclobutoxide were photodetached at 532 nm. The ground state of the cyclopropoxy radical has stable and dissociative components, while the first excited state is completely dissociative. These results showed that photodetachment from the a″ O σ_{2p} orbital in cyclopropoxide produces a more stable electronic configuration than photodetachment from the a′ O σ_{2p} orbital. The ground state of the cyclobutoxy radical is completely dissociative, suggesting that the interaction between the O σ_{2p} orbitals with the orbitals in the cycloalkyl moiety does not stabilize the cyclobutoxy radical [17].

In the current study, photodetachment of cyclopentoxide at 532 and 355 nm to the stable neutral radical and dissociative photodetachment (DPD) to 3-oxopropan-1-yl and ethylene was observed. Ab initio calculations on cyclopentoxide and 3-oxopropan-1-ide and the corresponding radicals aided in the determination of the dissociation energetics. The dissociation energies of cyclopentoxide and cyclopentoxy radical and the adiabatic electron affinity of cyclopentoxy radical constitute the first reported spectroscopic and thermodynamic data for cyclopentoxide.

2. Experiments

The fast-ion-beam photoelectron–photofragment coincidence spectrometer used in these experiments is only briefly reviewed here [18]. A space-focusing detection assembly [19] permits imaging of the photoelectrons in coincidence with the photofragments as in the cyclopropoxide and cyclobutoxide photodetachment experiments [17]. The energy and angular distributions of the photoelectrons are obtained from the position and time information.

Spectro-grade cyclopentanol (Acros, 99+%) seeded in a 10% mixture of N_2O in Ar produced anions in a pulsed discharge ion source. The anions were accelerated to 3 keV and the mass-selected beam at m/e 85 was intersected by the linearly polarized second (532 nm, 2.33 eV) or third (355 nm, 3.49 eV) harmonic of a Nd:YAG laser. The photodetached electrons are extracted in a 1.5 V/mm field toward a time- and position-sensitive detector [17]. The x- and y-velocity components of the photoelectron in the center-of-mass frame are determined relative to the center of the two-dimensional image. The limiting factor in the energy resolution is the z-velocity component, which is determined by the nominal photoelectron time-of-flight (TOF) of a few ns. The laser pulse width and uncertainties in measuring the TOF dominate the resolution, as do effects from the deflection of the incoming ion beam by the extraction field. The electron kinetic energy (eKE) in the CM frame is calculated from the three-dimensional recoil velocity. Calibration with O^- shows that the overall energy resolution is $\Delta E/E \sim 12\%$. Examining photoelectrons with minimal z-velocity components yields higher resolution, $\Delta E/E \sim 8\%$. Photoelectron spectra for cyclopentoxide were recorded in coincidence with m/e 85 photofragments and with $C_3H_5O + C_2H_4$ photofragments.

The photofragments from DPD events were detected by the photofragment translational spectrometer. The fragments recoil out of the beam over a 96 cm flight path and impinge upon a time- and position-sensitive detector after clearing a 7 mm wide horizontal beam stop. An electrostatic deflector removes residual anions from the beam. Conservation of linear momentum between photofragment pairs permits the determination of fragment masses and confirms that both fragments originated from the same dissociation event. The product masses cannot be assigned from the mass spectrum alone since resolution is limited to $m/\Delta m < 15$ [20]. The cyclopentoxy radical structure and the energetics of potential dissociation pathways are considered.

Like the dissociation of cyclopropoxy and cyclobutoxy, the dissociation of cyclopentoxy into 3-oxopropan-1-yl radical and ethylene involves simple C–C bond fission and the formation of a stable, unsaturated hydrocarbon and is expected to be favored over pathways involving bond rearrangements. The center-of-mass translational energy release, E_T, is calculated after the product masses are assigned. Contributions from false coincidences are estimated at ~5% [21].

3. Calculations

Ab initio calculations were carried out with the GAUSSIAN 98 program suite [22] on the Cray PVP cluster at the National Energy Research Scientific Computing Center (NERSC). Single reference geometry optimizations and normal mode analyses were performed at the MP2 [23] level of theory on the ground states of cyclopentoxide, cyclopentoxy radical, 5-oxopentan-1-ide, 3-oxopropan-1-ide and 3-oxopropan-1-yl radical. The Pople valence triple-ζ basis set [24] including diffuse and polarization functions on the heavy atoms (6-311+G*) was used, to maintain consistency with the calculations performed previously on cyclopropoxide and cyclopropoxy radical. The diffuse functions are required to accurately compute the absolute energy of the anionic species. Since the perturbative energies are not bound by the exact solution to the wavefunction, the energetics were computed at the optimized MP2 geometries with single point QCISD calculations [25] and are reported in Table 1.

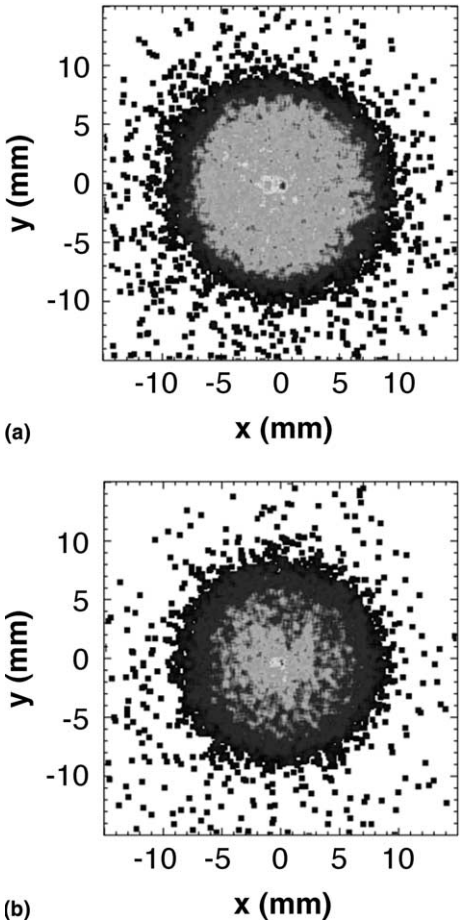

Fig. 1. Photoelectron images from cyclopentoxide photodetachment. Images of electrons detected in coincidence (a) with one neutral fragment, stable or dissociative, and (b) with two dissociative fragments. The laser polarization is perpendicular to the photoelectron detector face in (a). Since the angular distribution is isotropic, both parallel and perpendicular polarizations are included in (b).

Table 1
Relative energies (in eV) for participating species in cyclic alkoxide photodetachment, calculated with the 6-311+G* basis

	HF	MP2	QCISD	Exp
AEA (c-C_3H_5O)	−0.26[a]	1.29[a]	1.03[a]	1.424 ± 0.006[b]
T_0 (c-C_3H_5O)	0.23[a]	0.55[a]	0.43[a]	0.741 ± 0.002[b]
AEA (c-C_4H_7O)				1.7 ± 0.1[a]
AEA (c-C_5H_9O)	−0.17	1.74	1.38	1.5 ± 0.1
AEA (3-oxopropan-1-yl)	−1.17	0.33	0.15	–
ΔE (c-$C_5H_9O^-$-5-oxopentan-1-ide)	1.42	1.65	1.60	–

[a] Ref. [17].
[b] Ref. [31].

4. Results

Cyclopentoxide undergoes photodetachment to both stable and dissociative products at both 532 and 355 nm. The 532 nm spectra are reported here, as no new features were observed at 355 nm. In Fig. 1a, an image of photoelectrons from all photodetachment events was obtained by removing the beam block and requiring coincidence with one neutral photofragment. Fig. 1b shows an image of photoelectrons from dissociative photodetachment events only, obtained by requiring coincidence of the photoelectron with two momentum-matched neutral photofragments. Dissociation events account for less than 10% of the total, according to the ratio of intensities in the time-of-flight signal on the photofragment detector. The photoelectron angular distributions were nearly isotropic, as evidenced by the similarity of images taken at parallel and perpendicular polarizations of the electric vector to the detector face and the energy-dependent anisotropy parameter, $\beta(\mathrm{eKE}) \approx 0$.

The three photoelectron spectra of cyclopentoxide in Fig. 2 permit a comparison of the features depending on the types of photodetachment events. In Fig. 2a, the spectrum was recorded in coincidence with one photofragment. Fig. 2b was recorded in coincidence with either stable cyclopentoxy or ring-opened 5-oxo-pentan-1-yl radicals, identified as single photofragments impinging on the heavy particle detector at the beam velocity. Fig. 2c was recorded in coincidence with two dissociative photofragments only.

The contour map in Fig. 3 contains the photoelectron–photofragment kinetic energy correlation spectrum, $N(E_\mathrm{T}, \mathrm{eKE})$, of cyclopentoxide. Since the kinetic energies of the photoelectrons and photofragments from each dissociation event are recorded in coincidence, the plot shows how the available energy is partitioned during the dissociation process. The photoelectron spectrum, $N(\mathrm{eKE})$, and the photofragment translational energy spectrum, $N(E_\mathrm{T})$, are displayed on the x and y

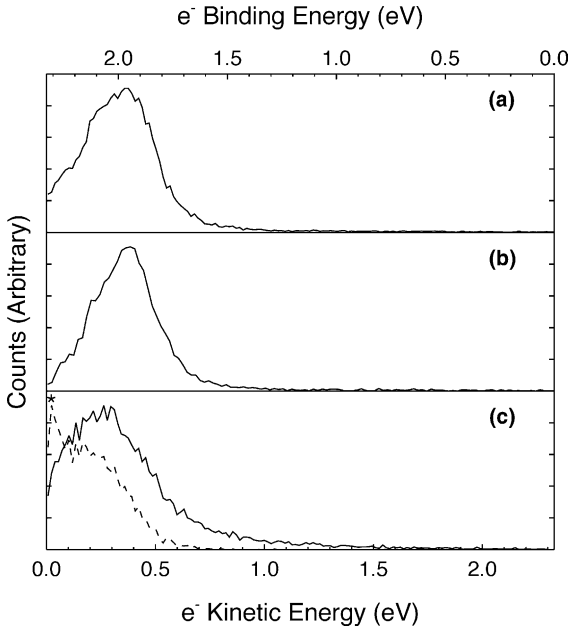

Fig. 2. Photoelectron spectra from cyclopentoxide photodetachment in coincidence (a) with one neutral fragment, stable or dissociative, (b) with cyclopropoxy and (c) with two dissociative fragments. The dashed curve in (c) shows the photoelectrons with minimal z-velocity components. The ZEKE peak is marked with an asterisk.

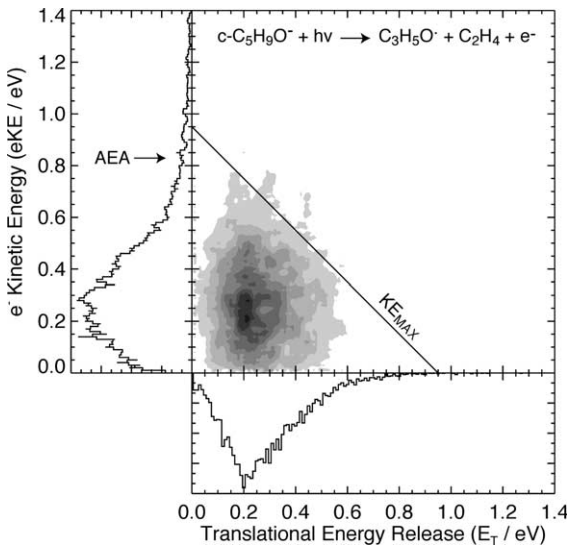

Fig. 3. Photoelectron–photofragment kinetic energy correlation spectra ($N(E_\mathrm{T}, \mathrm{eKE})$) of cyclopentoxide. The photoelectron spectrum ($N(\mathrm{eKE})$) and the photofragment translational energy spectrum ($N(E_\mathrm{T})$) are shown on the x- and y-axes, respectively. Integration of the correlation spectrum over the conjugate variable yields the one-dimensional spectra.

axes, respectively. The $N(E_T)$ distribution peaks at 0.20 ± 0.05 eV.

5. Discussion

5.1. Photoelectron spectra and images

In the cyclopentoxide spectra and images taken at 532 nm, there are two distinct energetic features. One is the broad feature corresponding to photodetachment to both stable and dissociative products in the range of eKEs between 0.1 and 0.9 eV. The other feature, between 0 and 0.1 eV, produces a bright spot at the center of the photoelectron images and a sharp peak in the photoelectron spectrum taken in coincidence with dissociative photofragments. In Fig. 2b the stable photoelectron spectrum peaks at $eKE = 0.38$ eV, corresponding to a vertical detachment energy (VDE) of 1.95 eV. In Fig. 2c, for dissociative products only, the VDE shifts to 2.05 eV, indicating that larger internal excitation in the stable radicals leads to increased dissociation. The lack of resolution in the spectrum precludes accurate assignment of the AEA, however, the adiabatic electron affinity (AEA) of 1.5 ± 0.1 eV is estimated from the broad feature at higher eKEs. The consistency of this value with the ab initio energetics obtained from MP2 and QCISD calculations for cyclopentoxide and the ground state of cyclopentoxy radical (Table 1) provides support for the estimation. The ZEKE peak, marked with an asterisk in Fig. 2c, cannot be unambiguously assigned. The feature may arise from a vibrational transition in the ground state or the first excited state of the cyclopentoxy radical.

5.2. $N(E_T, eKE)$ correlation spectrum and energetics

In Fig. 3, the dissociative photodetachment events are constrained by conservation of energy to lie within the triangle formed by the x and y axes and the maximum available kinetic energy, KE_{MAX}. This yields an accurate measure of the energy required for dissociative photodetachment with the assumption that the anion vibrational temperature is ≈ 0 K after being cooled by the supersonic expansion and that some of the dissociated fragments are formed with no internal excitation. Contributions from hot bands and the presence of minor isomeric forms of the anion cannot be ruled out owing to the lack of vibrational resolution. In addition, significant internal energy is expected in the polyatomic products. With these caveats in mind, the diagonal line along the 5% contour provides our best value for $KE_{MAX} = 0.95 \pm 0.07$ eV. The $N(E_T)$ distribution in the dissociation of cyclopentoxy radical peaks lower than in cyclopropoxy and cyclobutoxy at 0.20 ± 0.05 eV. This could be due to smaller repulsion between the neutral fragments or greater partitioning of the available energy to internal degrees of freedom.

In our previous study of cyclopropoxy and cyclobutoxy, the photon energy, KE_{MAX}, and AEAs of the cyclic alkoxy and product radicals were used to determine the dissociation energies of the cyclic alkoxide and alkoxy radical with respect to the dissociated products [17]. In the case of cyclopentoxy, the AEA of the dissociation product, 3-oxopropan-1-yl, has not previously been measured. This is required to determine the dissociation energy of the anion from the dissociative photodetachment data. Geometry optimizations and normal mode analyses were performed on both the 3-oxopropan-1-ide anion and 3-oxopropan-1-yl radical. The resulting absolute energies corrected by zero point energies were used to calculate the AEA. Since 3-oxopropan-1-yl is the ring-opened form of cyclopropoxy, the small values of the calculated AEAs in Table 1 are supported by the assignment of the broad feature at high eKE in our previous study of the stable cyclopropoxide photoelectron spectrum to photodetachment from the ring-opened carbanion, 3-oxopropan-1-ide [17]. The resulting energetics, summarized in Fig. 4, show that dissociation of cyclopentoxide into 3-oxopropan-1-ide and ethylene is strongly thermodynamically unfavorable. The ab initio results for the AEA of 3-oxopropan-1-yl yields dissociation energies, $D_0(\text{c-}C_5H_9O^-)$, of 1.05 ± 0.07 eV using the MP2 value and 1.23 ± 0.07 eV using the QCISD value.

The dissociation energy of the cyclopentoxy radical determined directly from the experimental

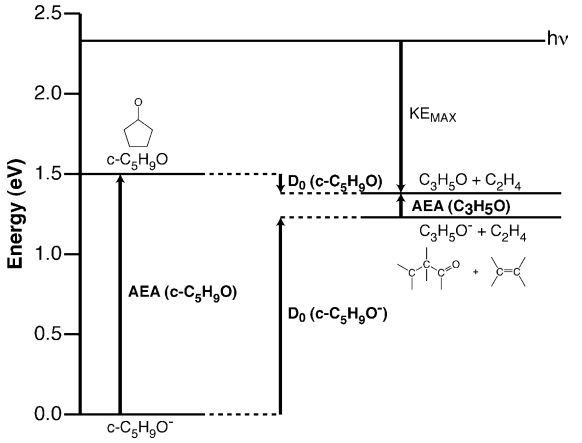

Fig. 4. Potential energy diagram, with energies in eV, for the species involved in cyclopentoxide photodetachment. Energy differences are from Table 1 and discussed in the text.

values, $D_0(\text{c-}C_5H_9O) = -0.12 \pm 0.12$ eV, shows that the radical is slightly thermodynamically unstable relative to dissociation products 3-oxopropan-1-yl and ethylene. This cannot be compared to literature values, as there have been no direct measurements of the heat of formation of the cyclopentoxy and 3-oxo-propan-1-yl radicals. An estimation of these quantities from the heats of formation of cyclopentanol, [1] propanal [26], the hydrogen atom [1] and typical RO–H and C–H bond energies in alcohols [27] and aldehydes [28], however, indicates that the dissociation is expected to be 0.4–0.6 eV endothermic. This discrepancy requires further experimental and theoretical investigation, with particular focus on verifying the energetics of these radicals and ruling out the presence of isomeric anions in this experiment.

Kinetic studies of cyclopentoxy radicals found that ring-opening is the dominant initial decomposition step under atmospheric conditions with a low barrier to ring-opening (<0.45 eV) [29]. Houk and co-workers [30] have calculated that the ring-opened 5-oxopentan-1-yl radical is 0.19 eV more stable than the cyclopentoxy radical. These results are consistent with the energetic shift observed between the stable and dissociative photoelectron spectra, although our results suggest that the radicals produced by photodetachment can dissociate from all levels of the ground state. Fig. 5 shows the possible dissociation mechanisms of the cyclopentoxy radical. Fig. 5a illustrates the stepwise dissociation discussed above. After ring opening, the 5-oxopentan-1-yl radical undergoes 2,3 C–C bond fission to produce ethylene (C_2H_4, $m/z = 28$) and the 3-oxo-propan-1-yl radical ($OCHCH_2CH_2$, $m/z = 57$). The two alternative mechanisms illustrated in Fig. 5b, c result from a 1,5 hydrogen transfer in the 5-oxopentan-1-yl radical, yielding the 1-oxopentan-1-yl radical. Fission of the 2,3 C–C bond in 1-oxopentan-1-yl (Fig. 5b) produces ketene (H_2CCO, $m/z = 43$) and the *n*-propyl radical ($CH_2CH_2CH_3$, $m/z = 42$). This pathway can be discounted since the photofragment mass distribution indicates $m/z = 57$ and $m/z = 28$ products. Fission of the 3,4 C–C bond in 1-oxopentan-1-yl (Fig. 5c) yields a diradical, 1-oxopropan-1,3-yl, ($OCCH_2CH_2$, $m/z = 56$) and ethyl radical (CH_2CH_3, $m/z = 29$). The experimental mass resolution does not permit elimination of this pathway by the fragment masses. However, the production of diradical and radical fragments is not expected to be energetically favorable. A hydrogen bond shift in the diradical would yield the stable product propenal ($OCHCHCH_2$), but this is yet another bond rearrangement. In contrast to these mechanisms, the dissociation mechanism shown in Fig. 5a yields stable products that have the correct mass ratio.

5.3. Comparison of cyclic alkoxy species

Notably absent from the images and the stable photoelectron spectrum of cyclopentoxide is a broad, low intensity feature at high eKE. This feature was observed in the cyclopropoxide data and was attributed to photodetachment from the isomeric ring-opened carbanion form of the cyclic species. According to the ab initio results (Table 1), cyclopentoxide is considerably more stable than the ring-opened carbanion, 5-oxopentan-1-ide. In contrast, calculations on cyclopropoxide and 3-oxopropan-1-ide showed those species to be comparable in energy. It is likely that photodetachment from 5-oxopentan-1-ide does not occur

[1] NIST Chemistry WebBook, http://webbook.nist.gov/, 2002.

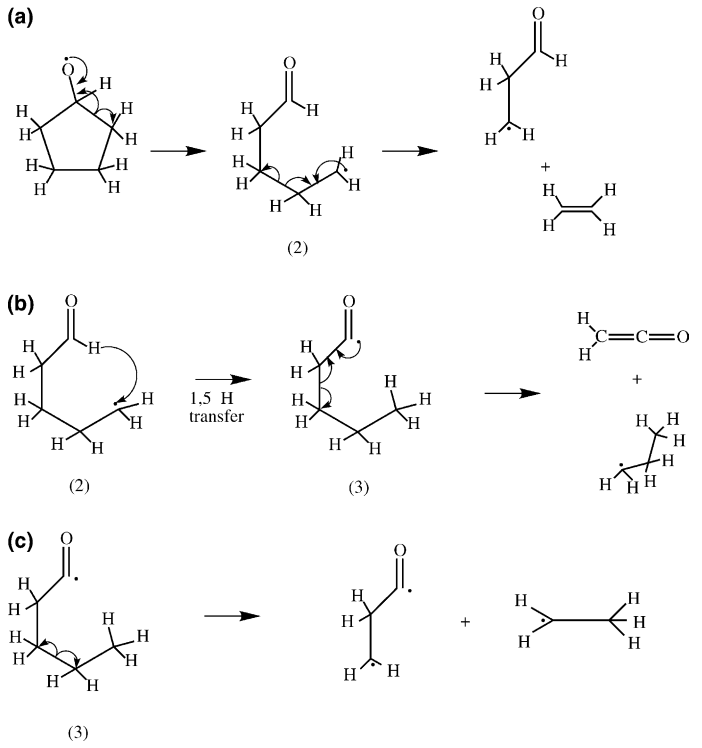

Fig. 5. Mechanisms for the unimolecular decomposition of the cyclopentoxy radical. Scheme (a) shows the dissociation into ethylene + 3-oxo-propan-1-yl proposed in the text. Schemes (b) and (c) are potential pathways involving 1,5 H transfer in the ring-opened 5-oxo-pentan-1-yl radical (2).

and photodetachment from cyclopentoxide alone was observed in this study.

The photoelectron spectra of cyclopentoxide obtained at a photon energy of 3.49 eV did not show additional features. If the transition to the first excited state had not already occurred, the separation between the ground and first excited states would be greater than 2 eV. The HOMO and the HOMO $-$ 1 of cyclopentoxide are the doubly occupied a$''$ and a$'$ oxygen lone pair σ_{2p} orbitals. Photodetachment from these two orbitals in many alkoxide species generally produces electronic configurations in the alkoxy radicals with small separation energies, less than or around 1000 cm^{-1} [27]. Interaction with other orbitals in the molecule can stabilize one configuration with respect to the other, increasing the separation energy, as in cyclopropoxy where $T_0 = 0.741$ eV. In cyclopropoxy, the dramatic energy difference between electronic configurations is attributed to the conjugation of the oxygen lone pair σ_{2p} orbitals with the sp^2 hybridized ring orbitals. These molecular orbital interactions are not expected in cyclopentoxy since the ring bonding orbitals in cyclopentyl lie along the bond direction and are sp^3 hybridized. Such molecular orbital interactions would not provide more than 2 eV of stabilization to either electronic configuration resulting from photodetachment from the HOMO or HOMO $-$ 1 of cyclopentoxide. Thus, it is probable that the transition to the first excited state of cyclopentoxy occurs but was not resolved in these spectra.

6. Conclusion

The stable and dissociative photodetachment processes of cyclopentoxide were studied at 532 and 355 nm. The dissociation energies of cyclopentoxide and cyclopentoxy radical were deter-

mined from the experimental and theoretical results. The alleviation of ring strain in the cyclopentyl moiety results in photodetachment and dissociation processes that are not dominated by electronic structure considerations as they are in the cyclopropoxy and cyclobutoxy radicals. Future threshold photodetachment studies should yield high resolution photodetachment spectra, providing more detailed information on the energetics of these interesting radicals.

Acknowledgements

This work was supported by the Chemistry Division of the National Science Foundation (CHE-0136195) and a grant of computer time from the National Energy Research Scientific Computing Center.

References

[1] R. Atkinson, Int. J. Chem. Kinet. 29 (1997) 99.
[2] C.A. Coulson, W.E. Moffitt, Philos. Mag. 40 (1949) 1.
[3] A.D. Walsh, Trans. Faraday Soc. 45 (1949) 179.
[4] J.F. Liebman, A. Greenberg, Chem. Rev. 76 (1976) 311.
[5] D.-K. Pan, J.-N. Gao, H.-L. Lin, M.-B. Huang, W.H.E. Schwartz, Int. J. Quantum Chem. 29 (1986) 1147.
[6] T. Egawa, T. Fukuyama, S. Yamamoto, F. Takabayashi, H. Kambara, T. Ueda, K. Kuchitsu, J. Chem. Phys. 86 (1987) 6018.
[7] Y. Endo, C. Man Chai, E. Hirota, J. Mol. Spectrosc. 126 (1987) 63.
[8] B.L. Liu, D.S. Kang, J. Chem. Inform. Comput. Sci. 34 (1994) 418.
[9] S. Inagaki, Y. Ishitani, T. Kakefu, J. Am. Chem. Soc. 116 (1994) 5954.
[10] P.B. Karadakov, J. Gerratt, D.L. Cooper, M. Raimondi, J. Am. Chem. Soc. 116 (1994) 7714.
[11] C.Y. Zhao, Y. Zhang, X.Z. You, J. Phys. Chem. A 101 (1997) 5174.
[12] T. Dudev, C. Lim, J. Am. Chem. Soc. 120 (1998) 4450.
[13] C.J. Hagedorn, M.J. Weiss, T.W. Kim, W.H. Weinberg, J. Am. Chem. Soc. 123 (2001) 929.
[14] K.B. Wiberg, Angew. Chem. Int. Ed. Engl. 25 (1986) 312.
[15] W.J. Adams, H.J. Geise, L.S. Bartell, J. Am. Chem. Soc. 92 (1970) 5013.
[16] H. Seong Jun, K. Young Kee, Theochem 362 (1996) 243.
[17] L.S. Alconcel, H.J. Deyerl, M. DeClue, R.E. Continetti, J. Am. Chem. Soc. 123 (2001) 3125.
[18] K.A. Hanold, R.E. Continetti, Chem. Phys. 239 (1998) 493.
[19] J.A. Davies, J.E. LeClaire, R.E. Continetti, C.C. Hayden, J. Chem. Phys. 111 (1999) 1.
[20] R.E. Continetti, in: C.Y. Ng (Ed.), Photoionization and Photodetachment, World Scientific, Singapore, 2000, p. 748.
[21] R.E. Continetti, Int. Rev. Phys. Chem. 17 (1998) 227.
[22] M.J. Frisch et al., GAUSSIAN 98, Gaussian, Inc, Pittsburgh, PA, 1998.
[23] C. Moller, M.S. Plesset, Phys. Rev. 46 (1934) 618.
[24] R. Krishnan, J.S. Binkley, R. Seeger, J.A. Pople, J. Chem. Phys. 72 (1980) 650.
[25] J.A. Pople, M. Head-Gordon, K. Raghavachari, J. Chem. Phys. 87 (1987) 5968.
[26] K.B. Wiberg, L.S. Crocker, K.M. Morgan, J. Am. Chem. Soc. 113 (1991) 3447.
[27] T.M. Ramond, G.E. Davico, R.L. Schwartz, W.C. Lineberger, J. Chem. Phys. 112 (2000) 1158.
[28] D.F. McMillen, D.M. Golden, Ann. Rev. Phys. Chem. 33 (1982) 493.
[29] J.J. Orlando, L.T. Iraci, G.S. Tyndall, J. Phys. Chem. A 104 (2000) 5072.
[30] S. Wilsey, P. Dowd, K.N. Houk, J. Org. Chem. 64 (1999) 8801.
[31] S.M. Casey, Ph.D. thesis, University of Minnesota, 1993.